Phase transitions of argon multilayer films on graphite: Evolution from multilayer film to bulk solid

J. Z. Larese and Q. M. Zhang
Chemistry Department, Brookhaven National Laboratory, Upton, New York 11973
(Received 30 December 1994; revised manuscript received 9 March 1995)

Using both high-resolution vapor-pressure isotherm and synchrotron x-ray scattering techniques, the evolution of the film-gas interface of multilayer argon on graphite with the film thickness has been explored. It is shown that an order-disorder transition occurs at the surface layer. The disordering of the surface layer with temperature can be described by an Arrhenius law. The maximum density change associated with the order-disorder transition of the top layer increases progressively with film thickness. This behavior may reflect the fact that a liquid layer is thermodynamically unstable at the bulk solid-gas interface below the premelting temperature.

I. INTRODUCTION

A central issue in the study of multilayer absorbed films is understanding the process by which a monolayer, a two-dimensional (2D) system, evolves into a three-dimensional (3D) system. This progression not only involves changes in the morphology of the film as a whole, but can also result in modification of the gas-film interface as well. The behavior of this interface with film thickness has been investigated theoretically[1] using a lattice-gas model. These studies suggest that at low temperature, a layer-by-layer growth of the film occurs through a series of discrete *first-order* layering transitions. Increasing the temperature eventually terminates this series of transitions at the nth layer at a temperature $T_c(n)$, referred to as the layering critical temperature. Beyond this point, film growth becomes continuous, characterized by the simultaneous population of atoms in the $n+1, n+2, \ldots$, etc., layers: i.e., film growth proceeds without additional discrete layering transitions.[2,3] They also suggest that as $n \rightarrow \infty$, $T_c(n)$ of a multilayer film approaches the roughening transition of the corresponding plane of the bulk crystal surface.[2,4] Although successfully relating the bulk roughening transition to a multilayer film surface transition, the models fall short of properly describing surface melting phenomena. This is primarily because they only allow for the presence of two phases (i.e., solid and vapor). It is evident from experimental studies, however, that a wide variety of physical changes occur at both the bulk surface and in multilayered films, which indicates the presence of a liquid or liquidlike phase as well. These changes include surface premelting,[5] layer-by-layer melting, surface reconstruction,[6] etc. All three thermodynamic states are needed not only to describe multilayer systems, but to understand the relationship between liquidlike behavior and multilayer film growth and the resulting phase diagram. We report here the results of a detailed experimental study of multilayer argon films adsorbed on graphite, which follows the changes in film properties with increasing thickness and explores the effects of the bulk interfacial properties on the surface phase diagram of the multilayer film.

The physical properties of multilayer argon films on graphite have been investigated by several groups. Their results are briefly summarized below. Heat capacity studied by Zhu and Dash[7] and more recently by Day *et al.*,[8] reported an anomaly near 68 K (nominally coverage independent), which they attributed to the layering critical point for multilayer films. Above that temperature, additional heat-capacity features were discovered which, for films four layers thick or less, could be attributed to discrete layer-by-layer melting. For thicker films, evidence of the surface premelting of bulk crystallites was also reported. Neutron-scattering experiments[9] and computer-simulation studies[10,11] provided microscopic evidence that supported Zhu and Dash's layer-by-layer melting scheme for films below four layers as well as the inference that bulk crystallites are present at greater coverages. Recently, an interesting ellipsometric isotherm study by Youn and Hess[12] (YH) reported that at temperatures above 73 K (i.e., is above the layering critical temperature reported by Zhu and Dash, and Day *et al.*), an unexpected resharpening of the growth steps occurs. YH associated these new features with the fourth, fifth, and sixth argon layers and attributed them to an unidentified reentrant first-order layering transition.

II. EXPERIMENTAL DETAILS

In an earlier paper[13] we presented a brief summary of our combined scattering, thermodynamic, and computer-simulation investigation of this reentrant phenomena. Here we discuss in more detail both the high-resolution vapor-pressure isotherm and synchrotron x-ray scattering portions of the experimental results for argon multilayer films on graphite. Descriptions of the procedure used in preparation of the graphite foam (Union Carbide) sample and of the high-resolution vapor-pressure isotherm apparatus have been presented elsewhere.[14] The x-ray experiment was performed at beamline X7B of the National Synchrotron Light Source at Brookhaven National Laboratory. The wavelength used was 0.9965 Å; data were collected in transmission. The instrumental resolution was about 0.005 $Å^{-1}$ and the temperature stability was better than 0.05 K.

III. EXPERIMENTAL RESULTS

A total of 20 isotherms were measured in the temperature range between 62 and 87 K (bulk triple point of argon T_m is 83.8 K). We intentionally restricted our investigations to a maximum surface coverage of five atomic layers in order to avoid complications associated with capillary-condensed bulk argon, which occurs at higher coverages in graphite foam. Plotted in Fig. 1(a) are several representative isotherms. As is customary, a 74.0 K nitrogen isotherm is used to define the coverage unit n quoted in the figure. A detailed analysis of the isotherms makes it possible to divide the behavior of the argon/graphite surface phase diagram into four distinct regions as a function of temperature. Below we briefly describe the general features associated with each region.

A. Isotherms

At low temperatures (region I), the isotherms exhibit abrupt, well-defined layering transitions. This is illustrated by the nearly vertical steps in the vapor-pressure data. At higher temperatures (region II), these sharp, discrete layering transitions terminate at the corresponding critical layering transition temperature $T_c(n)$. The values of the $T_c(n)$'s were taken to be the temperatures at which the slopes of the vertical step in the isotherms started to decrease. Thus, the second-layer critical temperature $[T_c(2)]$ is found to be 70.0±0.3 K, and both $T_c(3)$ and $T_c(4)$ occur at 67.2±0.2 K. These T_c values are in close agreement with the results of earlier experiments.[8,12] Above $T_c(n)$ at argon coverages near layer completion an interesting anomaly occurs: structure appears in the high-resolution vapor-pressure measurements. Analysis of isotherms recorded in the immediate neighborhood of $T_c(n)$ indicates that the transition associated with these weak features is very gradual or continuous. At higher temperature, however, the anomalies associated with the third and fourth layers sharpen dramatically. We identify the region of the phase diagram where these weak features evolve into first-order transitions as region III. The crossover temperature (from region II to region III) for the third layer is at 72.5±0.2 K; the fourth layer is at 71.0±0.5 K. The anomaly associated with the second layer behaves differently, however. It first appears at 67.0 K, a temperature *below* $T_c(2)$, and, although it becomes more pronounced with increasing temperature, it never exhibits the abruptness usually associated with a first-order transition. Hence, there is no region III associated with the second layer. The final segment of the phase diagram, region IV, appears as the temperature approaches the bulk triple point. It is characterized by a broadening of the first-order transitions of the three and four layers films occurring in region III. In Fig. 1(b), we present a representative set of isothermal compressibilities that illustrates the general appearance and behavior of these anomalies as a function of temperature.

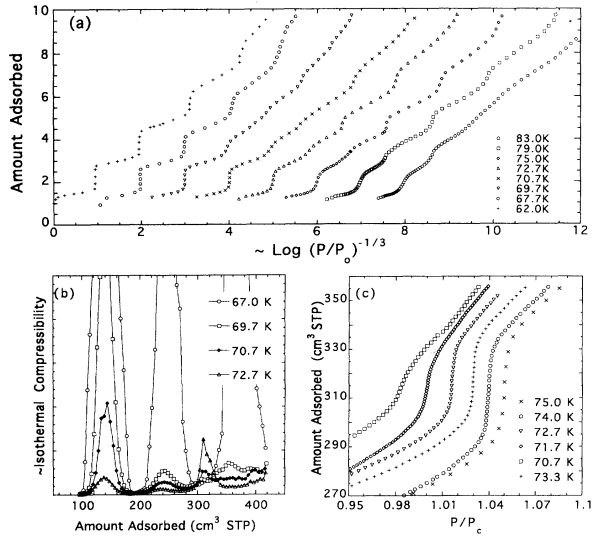

FIG. 1. (a) Representative isotherms of argon films adsorbed on graphite foam substrate. As noted in the text, the unit of coverage n is such that $n=1.0$ represents the number of molecules needed to complete a $\sqrt{3}\times\sqrt{3}R30$ commensurate nitrogen monolayer on the same substrate. This is not meant to be an indication that argon films form a commensurate solid with graphite. These units were employed so that direct comparisons with the data discussed here could be made at other laboratories. (b) Isothermal compressibility at several temperatures. Note that those traces that extend off-scale represent vertical steps in the isotherms. (c) Thermal evolution of the behavior of the isotherm step in the third-layer region of the phase diagram.

As we have noted earlier, the reappearance of the first-order-like behavior associated with region III was first observed by YH. Although they did not offer a detailed understanding of these features, they did discuss the relationship of their findings to a preroughening model proposed by den Nijs.[15] On the other hand, we have proposed an explanation[13] of the microscopic mechanism responsible for the reappearance of vertical isotherm steps based upon computer simulations and the experimental data presented here, which were not available at the time YH performed their initial experiments. We noticed that by carefully monitoring the thermal evolution of the anomalies observed in the second, third, and fourth layers, a subtle trend existed. First, all the anomalies appear at coverages above the corresponding layer condensation steps. In fact, they occur in a coverage regime that strongly resembles the argon *monolayer* phase diagram at temperatures above the 2D triple point.[16] These weak anomalies have been observed in the second-layer regime for Kr on graphite by Gangwar and Suter[17] and have been conjectured to exist by YH. Second, at higher temperatures, all connect to the freezing transition of the corresponding layer. We, therefore, tentatively identify the anomalies observed in region III with order-disorder (freezing) transitions of the topmost (nonsolid) layer of the multilayer film as it passes from a disordered or hypercritical-fluid phase back to a solid phase with increasing coverage. This identification relies, in part, on the similarities of the phase diagrams of the multilayer and monolayer systems. It is further supported by our previous neutron-diffraction studies, which showed that the topmost layer in an argon multilayer film starts to

disorder (melt) at temperatures near 67 K (Ref. 9) and by the results were reported earlier in our computer-simulation studies.[13] These earlier neutron measurements were carried out using a closed-cell arrangement (i.e., nominally constant coverage) and, therefore, followed a path through the phase diagram almost parallel to the temperature axis. The newly discovered features, on the other hand, are most readily observed along a path perpendicular to the temperature axis, i.e., one which involves *isothermal* increments in film thickness. What is clearly needed is a microscopic view of the transitions of interest. This we obtained by making synchrotron x-ray scans along several characteristic isothermal paths including 62.0 K (region I), 69.7 K (region II), and 73.0 K (region III). We restrict our subsequent discussion of the phenomena to those observed in the third layer only [see Fig. 1(c)]. The behavior of this layer is characteristic of the system as a whole in each of the three regions.

B. Diffraction

Figure 2 displays several typical x-ray diffraction traces. The diffraction profiles can be fitted using a composite, powder-averaged line shape: a Warren profile (modified for the multilayer effect[18]) to account for the solid portion of the film and, when needed, a broad Lorentzian profile of *fixed* (universal) width to account for the disordered-liquid component. The width of the Lorentzian used in these fits is determined by a fit to a characteristic fluid signal at high temperatures. The amplitude of this component is adjusted in order to account for the disordered component of the diffraction signal.

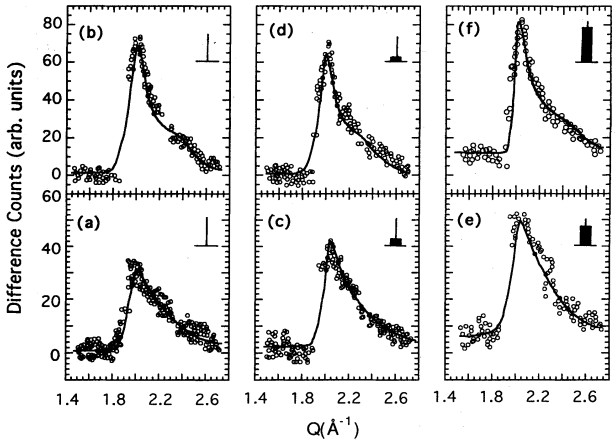

FIG. 2. Selected powder x-ray diffraction scans illustrating the coverage and temperature dependence of multilayer argon-on-graphite films. These traces are difference scans; i.e., the resultant of subtracting off a signal, which is recorded from a graphite-filled sample cell only. (a) $n=2.80$ and (b) $n=4.52$ were recorded at 62.0 K. (c) $n=2.96$ and (d) $n=4.74$ were recorded at 69.7 K. (e) $n=4.09$ and (f) $n=5.00$ were recorded at 73.0 K. Note that the vertical scales in the upper and lower halves of each panel are different. The bar-graph insets show the amplitude of the broad Lorentzian component used in the solid line and composite line shape fits to the data shown in the figures and discussed in the text.

[The *amplitude* of the disordered (fluid) component is indicated by the bar graph inset in each of the traces.] At 62 K, the diffraction profiles at $n=2.80$ and $n=4.52$ are well fitted, respectively, with a mutually commensurate solid bilayer and trilayer structures, reproducing our earlier neutron-scattering results[9] and indicating good thermal contact between the argon-graphite film system and the refrigerating surface. Another set of data was recorded at 69.7 K. At $n=2.96$ (i.e., just above the bilayer anomaly), the diffraction pattern indicates the existence of a commensurate bilayer solid film. When the coverage is further increased to $n=4.12$, which is above the third-layer condensation step (TC) but below the third-layer anomaly (TA), the diffraction pattern can no longer be fitted with a mutually commensurate trilayer solid. Instead, the scattered intensity is best fitted by assuming a commensurate bilayer and an independent single-layer solid structure indicating that the top solid layer is incommensurate with the bottom bilayer. Unfortunately, the interference of the graphite (002) peak at the leading edge of the lowest index film diffraction peak prevents a more quantitative statement about changes in the correlation length of the top layer. A small, but definite, increase in the scattered intensity observed at wave numbers (Q) below 1.8 Å^{-1} is, however, consistent with the appearance of some type of structural disorder in this coverage region. When the coverage is increased still further to $n=4.74$, which is above the trilayer anomaly, the diffraction data show that the film recovers its mutually commensurate trilayer solid structure. Thus, there is direct microscopic evidence that above and below the anomalies in the vapor-pressure isotherm a structural reordering occurs within the trilayer solid film. At 73 K (a temperature within region III), the diffraction data taken at $n=4.09$ (again a coverage above TC but below TA) indicate a marked increase in the scattered intensity at Q's below 1.8 Å^{-1} accompanied by a 15% decrease in the peak intensities compared to the 69.7-K data at the same coverage. Thus, the top layer is much more disordered at 73 than at 69.7 K. At $n=5.0$, the diffraction profile indicates that the solid portion of the film has returned to the mutually commensurate trilayer state. This observation is additional evidence that the small vapor-pressure isotherm anomalies, which steadily evolve into sharp steps, the "reentrant processes" of YH, are some form of order-disorder transition. In particular, the transition associated with region III most likely involves freezing (recrystallization) of the outermost layer of the trilayer film. The $n=5.0$ data also suggests that at temperatures *above* the layer critical point, an isothermal increase in the surface coverage may first result in a discommensuration of the outermost layer(s) of the film with respect to the bottom layer(s) before a more extensive lateral disordering occurs in the layer itself. The data also suggest that the attractive interaction of the overlayer with the substrate acts as a powerful mechanism for stabilization and recrystallization of the argon multilayer film.

IV. DISCUSSION

Let us now turn to a more detailed description of the order-disorder transition associated with each layer and

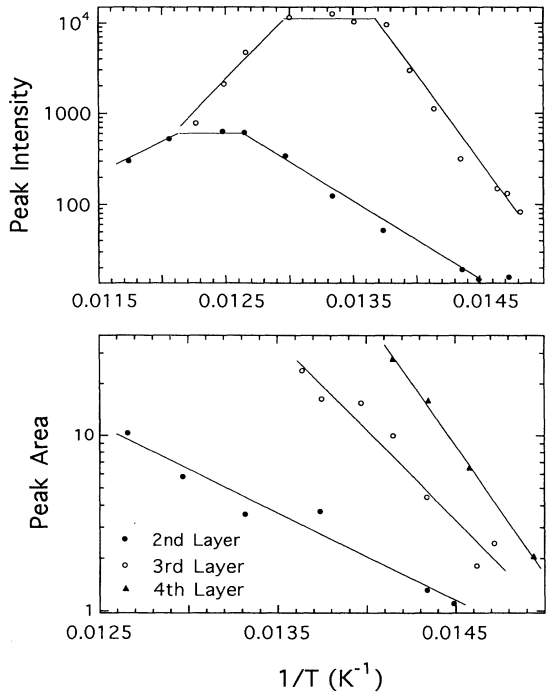

FIG. 3. Plots of the peak height (a) and area (b) vs $1/T$ for argon films adsorbed on graphite in the two-to-four–layer regime.

investigate how it changes with increasing film thickness. To analyze the evolution of this transition, we calculated $p(dn/dp)$ along several isotherms and then determined the anomalous density change *(peak area)* associated with the transitions. Representative data are shown in Fig. 3. The peak associated with the transition has a sawtooth shape [see Fig. 1(b)]. In the bilayer regime, this peak increases in magnitude with increasing temperature attaining a maximum height at 79 K, then leveling off until approximately 82 K, at which point the intensity drops and the peak broadens. Between 69 and 79 K both the peak height (PH) and the area (A) can be well described using an exponential function [$(\mathrm{PH}=A\exp(-E/k_BT)$]. This analysis indicates that an Arrhenius-type disordering process with a single activation energy occurs, possibly related to a defect creation mechanism. The region II behavior for both the three- and four-layer films is similar to that for the bilayer except that it appears over a narrower temperature interval. This similarity can be made more quantitative by noting the systematic increase with film thickness of the adjustable parameters, A_i and E_i, in the Arrhenius law. For bilayer films, the resulting fit of the peak area vs temperature yields $A_2=2.3\times10^7$, $E_2=1162k_BK$; for a trilayer film, $A_3=3.7\times10^{15}$, $E_3=2389k_BK$; and for a four-layer film, $A_4=7.5\times10^{21}$, $E_4=3325k_BK$. One notes that, as the film thickens, the activation energy associated with the defects increases steadily and, in particular, the number of defect sites (proportional to A) grows *significantly*. This result implies that although the order-disorder transition is mostly confined to the surface layer of the argon multilayer film, the underlying layers have an increasing influence on the transition as the number of layers grows.

V. CONCLUSIONS

In Fig. 4, we present a phase diagram for multilayer argon-on-graphite films. When combined with the earlier ellipsometric results of YH and the thermodynamic measurements of Zhu and Dash[7] and of Day *et al.*,[8] it suggests that the argon multilayer phase diagram has the same general form for each layer as the film thickness increases. Above the layering critical point, several important changes in film growth appear. These probably imply that above $T_c(n)$ film growth not only extends over several layers producing a broadened interface but that a simultaneous disordering of the topmost layer occurs as well. Thus, the data presented here suggest a simple microscopic interpretation of the reentrant first-order-layering transitions (i.e., of the reappearance of vertical isotherm steps) observed in region III. At low temperatures, i.e., in region I, below the layering critical point, the vertical isotherm steps indicate layer-by-layer growth involving the movement of the solid-vapor interface away from the graphite substrate. In region III, the x-ray diffraction scans indicate that the reappearance of the vertical isotherm step is associated with solid-fluid coexistence. We, therefore, are led to identify the reentrant behavior observed by YH with the appearance of a solid-fluid interface. Unlike the sharp solid-vapor interface of region I, the solid-fluid interface in region III is spatially extended normal to the film plane, especially as the temperature and film thickness increases. For example, we observe that the coverage width, dn, associated with the region III order-disorder transition increases from $dn\approx0.3$ in the bilayer region, to $dn\approx0.63$ in the trilayer region, and to $dn\approx0.8$ in the four-layer regime. This implies (for films with individual layer solid and liquid densities, which remain fairly constant during isothermal

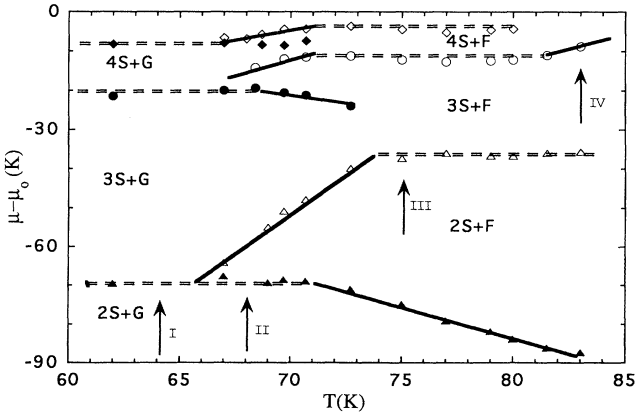

FIG. 4. Phase diagram for argon-on-graphite films from two-to-four layers thick. The symbols S, G, and F stand for solid, gas, and fluid, respectively. Hence $2S+F$ represents two solid layers plus fluid. Dashed lines indicate regions where vertical steps are recorded in the vapor-pressure isotherms.

growth) that atoms added to the cell in the reentrant region (III) adsorbed with a height profile, which extends increasingly far away from the outermost complete solid layer as the film thickness increases. In light of the fact that a bulk liquid layer is not an allowable thermodynamic state below the bulk melting temperature T_m, such behavior implies a broadened film interface with a decreasing mean density.

Although the presence of the graphite substrate limits direct applicability to the melting properties of bulk argon, these studies should serve to shed some light on the microscopic activity, which occurs near bulk melting transitions, and reemphasize the fact that theoretical models that seek to describe melting phenomena must intrinsically include all three thermodynamic states.

ACKNOWLEDGMENTS

We would like to express our appreciation to our many colleagues whom we have had extensive fruitful discussions with. In particular, we thank Professor James M. Phillips, Dr. Julius Hastings, and Dr. Laurence Passell for their active role in helping us develop our understanding of these systems. Professor George Hess, Professor Greg Dash, Professor Aldo Migone, Professor Marcel de Nijs, Professor Bill Steele, Professor Moses Chan, and Professor Ailan Chen have all had a positive impact on our thinking about these systems. This work was supported by the U.S. Department of Energy, Materials Science Division, under Contract No. DE-AC02-76CH-00016.

[1]M. J. de Oliveira and R. B. Griffiths, Surf. Sci. **71**, 687 (1978).
[2]R. Pandit, M. Schick, and M. Wortis, Phys. Rev. B **26**, 5112 (1982).
[3]Guozhong An and M. Schick, Phys. Rev. B **37**, 7534 (1988).
[4]J. D. Weeks, Phys. Rev. B **26**, 3998 (1982); D. A. Huse, *ibid.* **30**, 1371 (1984); M. P. Nightingale, W. F. Saam, and M. Schick, *ibid.* **30**, 3830 (1984).
[5]J. W. M. Frenken and J. F. van der Veen, Phys. Rev. Lett. **54**, 134 (1985); P. H. Fuoss *et al.*, *ibid.* **60**, 2046 (1988).
[6]Doon Gibbs *et al.*, Phys. Rev. B **38**, 7303 (1988).
[7]D. M. Zhu and J. G. Dash, Phys. Rev. Lett. **57**, 2959 (1986); **60**, 432 (1988).
[8]P. Day *et al.*, Phys. Rev. B **47**, 10 716 (1993).
[9]J. Z. Larese and Q. M. Zhang, Phys. Rev. Lett. **64**, 922 (1990); J. Z. Larese *et al.*, Phys. Rev. B **40**, 4271 (1989).
[10]A. L. Cheng and W. A. Steele, Langmuir **5**, 600 (1989).
[11]J. M. Phillips, Phys. Lett. A **147**, 54 (1990).
[12]H. S. Youn and G. B. Hess, Phys. Rev. Lett. **64**, 918 (1990); H. S. Youn, X. F. Meng, and G. B. Hess, Phys. Rev. B **48**, 14 556 (1993).
[13]J. M. Phillips, Q. M. Zhang, and J. Z. Larese, Phys. Rev. Lett. **71**, 2971 (1993).
[14]Q. M. Zhang and J. Z. Larese, Phys. Rev. B **43**, 938 (1991).
[15]M. den Nijs, Phys. Rev. Lett. **64**, 435 (1990).
[16]A. D. Migone *et al.*, Phys. Rev. Lett. **53**, 810 (1984).
[17]R. Gangwar and R. M. Suter, Phys. Rev. B **43**, 938 (1991).
[18]J. Z. Larese *et al.*, Phys. Rev. B **37**, 4735 (1988).